P-14

NASA Technical Memorandum 83439

Experimental Results for a Two-Dimensional Supersonic Inlet Used as a Thrust Deflecting Nozzle

Albert L. Johns and Paul L. Burstadt
Lewis Research Center
Cleveland, Ohio

Date for general release _____ July 1988

"Copy Control Number # 1 _____."

NASA

ORIGINAL CONTAINS
COLOR ILLUSTRATIONS

Copy # 1

EXPERIMENTAL RESULTS FOR A TWO-DIMENSIONAL SUPERSONIC INLET
USED AS A THRUST DEFLECTING NOZZLE

by Albert L. Johns and Paul L. Burstadt
National Aeronautics and Space Administration
Lewis Research Center
Cleveland, Ohio 44135

E-1737

ABSTRACT

Nearly all supersonic V/STOL aircraft con-
cepts are dependent on the thrust deflecting capa-
bility of a nozzle. In one unique concept,
referred to as the reverse flow dual fan, not only
is there a thrust deflecting nozzle for the fan
and core engine exit flow, but because of the way
the propulsion system operates during vertical
take-off and landing, the supersonic inlet is also
used as a thrust deflecting nozzle. This paper
presents results of an experimental study to eval-
uate the performance of a supersonic inlet used as
a thrust deflecting nozzle for this reverse flow
dual fan concept. Results are presented in terms
of nozzle thrust coefficient and thrust vector
angle for a number of inlet/nozzle configura-
tions. Flow visualization and nozzle exit flow
survey results are also shown.

SYMBOLS

AE	nozzle exit area, cm^2
AO	nozzle entrance area, cm^2
CFN	nozzle gross thrust coefficient: FN/FIDEAL
FIDEAL	thrust of measured mass flow exhausting at VIDEAL, kg
FN	measured thrust, kg
VIDEAL	velocity after isentropic expansion from average nozzle entrance conditions to ambient conditions, cm/sec
W7SPC	nozzle entrance weight flow corrected to local conditions/nozzle entrance area kg/cm^2-sec
PHI	nozzle thrust vector angle measured from the inlet/nozzle centerline, deg

INTRODUCTION

A unique propulsion system concept for super-
sonic V/STOL aircraft is discussed in Ref. 1. It
is referred to as the reverse flow dual fan con-
cept, and it uses the engine front inlet as a
thrust deflecting nozzle during vertical takeoff
and landing. This concept is similar to the more
familiar tandem-fan system described in Refs. 1
and 2. A schematic of the concept is shown in
Fig. 1. With the engine inlet being used as a
nozzle, the spacing between the fore and aft
thrust vectors is relatively large. This results
in two potential advantages for the concept.
First the propulsion system can be moved futher
rearward to a point where it integrates better
with the aircraft. Secondly, this rearward move-
ment of the propulsion system leads to more length
for installing the inlet which in turn permits the
use of a two dimensional inlet (as opposed to a
shorter axisymmetric inlet) with its inherently
better angle-of-attack performance.

A more detailed picture of the reverse flow
dual fan propulsion system is shown in Fig. 2 dur-
ing the vertical takeoff and landing mode, transi-
tion, and horizontal flight. The plus sign in
Fig. 2 denotes the fan blades in normal pitch and
the minus sign denotes the fan blades in reverse
pitch. In the vertical takeoff and landing modes
(fig. 2(a)), the front fan reverses its direction
of flow, whereupon the front fan inlet becomes the
front fan thrust deflecting exhaust nozzle. The
auxiliary inlet between the two fans must now pro-
vide airflow for not only the aft fan and core
engine, but also for the front fan which is flow-
ing in reverse.

In the transition mode (fig. 2(b)), the front
inlet/nozzle must overturn the airflow (>90°
deflection) while the aft nozzle deflection angle
is being reduced. In the horizontal flight mode
(fig. 2(c)), the front fan operates at normal
pitch, the inlet between the two fans is closed,
and the inlet/nozzle becomes a full-time inlet
providing airflow for both fans.

This paper presents the results of an experi-
mental study which used a two-dimensional super-
sonic inlet model as a thrust deflecting nozzle
for the reverse flow dual fan supersonic V/STOL
concept. The test was conducted in the NASA Lewis
Vertical Thrust Stand by mounting the compressor
face station of the supersonic inlet to the dis-
charge of a 30.5 cm (12 in.) diameter fan.

The NASA Lewis Research Center's program to
study deflected thrust V/STOL nozzles[3] has con-
centrated on a number of nozzle configurations
designed for the low pressure ratios typical of
the high bypass ratio turbofan engines suited for
subsonic aircraft. This paper deals with a super-
sonic V/STOL propulsion concept, but the parallel
operation of the engine's fan stages during take-
off and landing produces low nozzle pressure
ratios comparable to those of Ref. 3, and hence,
the results will be examined in a similar manner.

APPARATUS

Test Facility

The two-dimensional inlet/nozzle installed in
the NASA Lewis Research Center Vertical Thrust
Stand is shown in Fig. 3. The insert on Fig. 3
gives a close-in view of one of the inlet/nozzle
configurations that will be described shortly.

A schematic of the test apparatus and the
nozzle exit flow survey rake system is shown in
Fig. 4. The test apparatus consisted of an inlet
bellmouth, a 6-component force balance, a 30.5 cm
(12 in.) diameter tip-turbine driven fan, and a
two-dimensional supersonic inlet. The supersonic
inlet was modified to function as a thrust
deflecting nozzle.

A total pressure rake was located at the
nozzle entrance station. A traversing rake was
used to survey the deflected flow field at the
nozzle exit plane. The rake consists of 20 total

temperature probes and 21 flow angularity probes. The three-tube design of the flow angle probes measures total pressure and the angle in one plane, so the probe orientation alternates across the rake to obtain angles in the "pitch" and "yaw" planes. The rake support was attached to the non-metric portion of the thrust stand and allowed the rake to be translated in the vertical and horizontal directions, and rotated in the "pitch" plane. A six-component balance was used to measure the nozzle forces and moments.

Model Configurations

The three model baseline configurations are shown in Fig. 5 and are described as follows:

Circular arc deflector. - The circular arc deflector (fig. 5(a)), is representative of a flap which would be stored within the inlet compartment. For deployment, the flap would rotate down out of the ramp compartment. The deflector flap angle variation ranged from $90°$ to $110°$ as indicated in the figure. The deflection angle was measured with reference to the inlet centerline. The deflector axial position was also varied from 48.77 cm (19.20 in.) to 56.39 cm (22.20 in.) from the ramp leading edge.

Single-hinged deflector. - The single-hinged deflector (fig. 5(b)), is representative of the first ramp being rotated down for use as the deflecting flap. The deflector was located 33.53 cm (13.20 in.) from the ramp leading edge. The single-hinged deflector flap angle varied from $70°$ to $90°$ and had a length of 32.51 cm (12.80 in.).

Double-hinged deflector. - The double-hinged deflector (fig. 5(c)), was a modification of the single-hinged deflector concept. The double-hinged deflector allows the airflow to make a two stage turn. The first flap angle was varied from $60°$ to $80°$ and the second flap remained at a $90°$ deflection. The length of the first flap was 10.16 cm (4 in.), and 22.35 cm (8.8 in.) for the second flap.

Cowl lip droop was a variable for each of the baseline configurations. Four droop lip configurations were tested with the circular arc deflector, $0°$, $40°$, $70°$ and $90°$, as indicated in Fig. 5(a). The single-hinged deflector was tested with three lip configurations; $0°$, $40°$ and with the lip removed (this represented a retractable lip), as shown in Fig. 5(b). The double-hinged deflector was tested with a $40°$ and $90°$ droop lip (fig. 5(c)). The droop lips were an integral part of this supersonic inlet model and would be used for improved inlet performance at low speeds, at high angles-of-attack, and also during transonic maneuvers.

In addition to the baseline configurations shown in Fig. 5, several modifications were made and these are shown in Fig. 6. Although the modifications are shown only for the circular arc deflector these modifications were also applied to the single and double-hinged deflectors.

The modifications are as follows:

Sidewalls. - Sidewalls were added between the sideplates and deflector (fig. 6(a)). These sidewalls were intended to prevent the sideways flow of air at the nozzle exit.

Deflector tip extension. - The deflector tip was extended 12.9 cm (5 in.), Fig. 6(b). The extension provided more deflector surface for turning.

Ramps. - The two dimensional inlet had a $-8°$ ramp angle. Wedges of $8°$ and $18°$ were installed on the $-8°$ ramp which produced net ramp angles of $0°$ and $10°$. These wedges were added to eliminate diffusion along the ramp surface and to provide for some earlier turning of the flow (fig. 6(c)).

TEST PROCEDURE

Nozzle entrance test conditions were set by adjusting the valves which provided hot, high pressure air to the fan tip turbine. When data were being recorded to define the nozzle thrust vector and flow rate (performance data), the exit flow survey rake was moved to a position well away from the exhaust jet. Performance data were obtained over a range of nozzle pressure ratios that was limited by either the maximum speed or the stall limits of the fan. Force measurements at zero-flow conditions were recorded to determine model weight tares required in the determination of thrust.

Nozzle exit flow field data were obtained by setting the desired operating condition and then incrementally moving the servey rake across the exhaust jet. If necessary, the rotary position of the rake was varied at each location to minimize the angle of the flow with respect to the probes. The nozzle entrance conditions were measured at each rake position to account for minor variations of the desired operating condition.

PRESENTATION OF EXPERIMENTAL RESULTS

The nozzle thrust coefficient, CFN, is used as the primary measure of system performance and efficiency. In this program, all test were conducted at static conditions and CFN is a gross thrust coefficient determined by the measured thrust and mass-flow rate, and the ideal velocity. Since measured mass flow is used in the denominator, this coefficient may be interpreted as the ratio of actual-to-ideal velocity at the nozzle exit. Total pressure, total temperature, mass flow rate and area at the nozzle entrance are used to calculate a specific corrected airflow, W7SPC. The nozzle thrust vector angle is also used in the performance data plots. The nozzle thrust vector angle, PHI, is measured from the inlet centerline.

RESULTS AND DISCUSSION

The performance characteristics of the baseline configurations are shown in Fig. 7, for a $40°$ droop lip and $90°$ flap deflection angle. These results consist of the nozzle thrust coefficient and vector angle versus the nozzle specific corrected airflow. Data are shown for the circular arc and single and double hinged deflectors over a range of specific corrected airflows. In general, both the thrust coefficient and thrust vector angles were low for all three configurations.

The nozzle thrust coefficient was approximately 78 percent for the circular arc and 74 and 73 percent for the single-hinged and double-hinged deflectors, respectively. The nozzle thrust vector angle was approximately $48°$, $42°$, and $38°$ for the circular arc, double and single hinged deflectors.

The effect of drooping the cowl lip on the baseline circular arc deflector configuration is shown in Fig. 8. These results again consist of the nozzle thrust coefficient and thrust vector angle versus the nozzle specific corrected airflow. The results presented for the circular arc deflector are typical for the other configurations. As shown, increasing the lip droop angle from 0° to 40° and to 70° produced little change in thrust coefficient. Thrust coefficient ranged from 78 to 79 percent.

However, as indicated by Fig. 8(b), lip droop did effect the measured thrust vector angle. The thrust deflection angle was highest at about 55°, with the zero degree lip compared to about 48° for the 40° and 70° lips. The 0° lip apparently tends to maintain the nozzle inner flow within the plane of the deflector. This allows the deflector flap to force the airflow turning and produce a slightly higher turning angle. On the other hand the droop lips allow the nozzle inner flows to expand beyond the deflector tip, "miss" the deflector and hence result in a higher axial component and a lower deflecting angle. In general, however, drooping the cowl lip did not have a significant effect on nozzle performance either for the circular arc deflector configuration as shown here or for the other two configurations.

It is obvious from Figs. 7 and 8 that the performance of the three configurations in terms of both deflecting angle and nozzle thrust coefficient was relatively poor. In order to understand these results more thoroughly, a flow visualization test was conducted to determine the nature of the low thrust deflection angle and low performance. The flow visualization results are shown in Fig. 9 for all three configurations. The flow pattern on each deflector is unique. However, it is obvious from all the flow patterns that there is a significant amount of flow going out the sides of the nozzle. Sidewalls were added to prevent this out flow.

The effect of sidewalls on the nozzle performance characteristics is shown in Fig. 10 for the double-hinged deflector. Sidewalls were tested with the other two deflectors with similar results. The results shown in Fig. 10 are shown again in terms of nozzle thrust coefficient and thrust vector angle versus the nozzle specific corrected airflow. Results are shown both with and without sidewalls so a direct comparison can be made. The lip droop angle is different for the two configurations, but as was shown in Fig. 8, this has no significant effect on the nozzle thrust coefficient and only small effects on nozzle thrust vector angle.

In general, the nozzle thrust coefficient increased significantly, from approximately 0.73 to 0.84 and the nozzle thrust vector angle increased significantly from about 38° to 68°. These results were due to the comfinement and the directing of the nozzle exit flow provided by the sidewalls.

The sidewalls that were added were longer than the deflector flap. A flow visualization test was conducted to examine the flow patterns in the region of the deflector tip. These flow visualization results are shown in Fig. 11 for the double-hinged deflector. The deflector angle was 60° for the first segment and 90° for the second segment. Specific corrected airflow was 0.014 kg/cm²-sec. The paint flow on the sidewalls,

where it meets the deflector flap, indicates incomplete turning by the deflector, thereby suggesting a need to extend the deflector length. Therefore, the circular arc deflector tip was extended by 12.7 cm (5 in.) and the double-hinged deflector second flap was extended to 33.02 cm (13 in.). Results for the double-hinged deflector with extended flap are shown in Fig. 12 along with results without the extension.

The results again consist of the nozzle thrust coefficient and thrust vector angle versus the nozzle specific corrected airflow. The nozzle thrust coefficient showed a slight drop as a result of extending the flap, however, the thrust deflecting angle increased significantly from 60° to 76°. These results are also typical of the results obtained for the circular arc deflector. Hence, it appears that we are approaching the level of nozzle thrust vectoring angle needed. However, the nozzle thrust coefficient is still much lower than desired.

If we take a look at the flow visualization results shown in Fig. 13, there are two obvious problems that may remain. First, there are two vortices on the ramp and second, there is a region along the deflector flap where the flow is impinging directly with some flow deflected upward and some flow deflected downward. In an effort to reduce or eliminate the vortices and flow impingement, and at the same time increase the flow turning, ramps were added to "fill in" the diffusing ramp surface upstream of the deflector.

First, an +8° ramp insert was added to the -8° ramp (net angle of 0°), and tested with the double-hinged and cicular arc deflectors. The effect of the ramp on nozzle performance characteristics is shown in Fig. 14. As before the results are presented as a function of nozzle thrust coefficient and thrust vector angle versus the specific corrected airflow.

The double-hinged deflector (fig. 14(a)), was tested with the droop lip removed, with sidewalls, and with the extended deflector flap. In general, the 0° ramp had a thrust coefficient of approximately 86 percent as opposed to 84 percent for the -8° ramp. The nozzle thrust vector angle was 84° for the 0° ramp and 76° for the -8° ramp.

The circular arc deflector was also tested with the 0° and -8° ramps, 90° droop lip, sidewalls and extended deflector flap. The results are shown in Fig. 14(b). The nozzle thrust coefficient was approximately the same for both ramps, 82 to 83.5 percent. However, the 0° ramp had a nozzle thrust vector angle of 95° compared to 91° with the -8° ramp. The use of the 18° ramp insert (a net 10° ramp angle) resulted in only a slightly higher thrust vector angle. Hence, for the circular arc deflector configuration by adding sidewalls, the flap extension and the 8° ramp insert the performance was improved from baseline values of thrust coefficient and vectoring angle of 78 percent and 48° respectively, to 87 percent and 97°.

One last parameter investigated is nozzle exit area variation. The nozzle exit area was varied by changing the deflector axial position. The effect of nozzle exit area variation on the nozzle performance characteristics is presented in Fig. 15 for the circular arc deflector. Again, the nozzle thrust coefficient and thrust vector angle are shown versus specific corrected airflow. Two area ratios are shown, AE/AO of 1.361 and 1.05, at a flap deflection angle of 100° with the -8° ramp and the cowl lip removed. Both the

thrust coefficient and the nozzle thrust vector angle are highest with the large exit area with thrust coefficient as high as 87 percent and thrust vector angles of 97°.

To illustrate the extremes in nozzle performance, contour maps of the nozzle exit total pressure ratio are shown in Fig. 16 for the circular arc deflector. Nozzle exit total pressure has been ratioed to the average total pressure at the nozzle exit. Figure 16(a) shows the contour map for a baseline case, specific corrected airflow of 0.014 kg/cm^2 sec where the performance was relatively poor. In general, the exit flow occupies less than half of the nozzle exit area. Although, there is a region of high total pressure, a much larger extent of the region has low total pressure. The thrust coefficient and vector angle are low, 78 percent and 48°, respectively.

Figure 16(b) shows the pressure contour map for the circular arc deflector with the sidewalls and extended deflector flap added. In general, the high pressure region is considerably larger in extent, however, less than 75 percent of the nozzle exit plane is occupied by the flow. The nozzle thrust coefficient was approximately 84 percent (improved, but still low) with a thrust vector angle of 97°.

In summary, Fig. 17 shows results obtained for the two-dimensional inlet being used as a nozzle. The baseline configurations resulted in low nozzle thrust coefficient (fig. 17(a)), and vector angle (fig. 17(b)). Drooping the cowl lip had a minimal effect on the nozzle performance characteristics. The addition of sidewalls resulted in improved nozzle thrust coefficient with an increase of 30° in the nozzle thrust vector angle. Further improvements were obtained by extending the deflector flap and by the use of ramp angle variation. Once again, although results are summarized here only for the double-hinged deflector, they are also generally true for the circular arc and single-hinged deflector.

SUMMARY AND CONCLUDING REMARKS

The major results of an experimental study of a two-dimensional supersonic inlet used as a
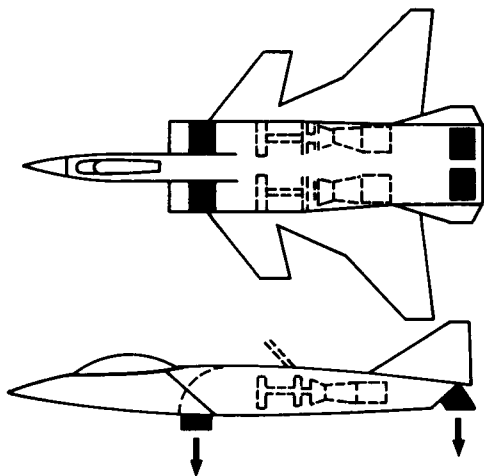
thrust deflecting nozzle for the reverse flow dual fan supersonic V/STOL concept are as follows:

1. For the three baseline nozzle configurations, the nozzle thrust coefficient was at best about 78 percent. By adding sidewalls, extending the deflector flap and adding a ramp insert, the thrust coefficient was improved to about 86 percent. This level is still less than that desired.

2. High nozzle thrust vector angles were obtained through addition of the modifications described above. Before the modifications, the best vector angle was about 48° and after, it was greater than 90°.

It is felt that the nozzle thrust coefficient could be improved further by starting the initial turning of the airflow further upstream inside the diffuser. Also a supersonic inlet would have bleed holes at the throat, on the ramp and possibly on the sideplates, which could be used for suction or blowing to remove or energize the boundary layer for improved performance. The above techniques when applied to the two-dimensional inlet/nozzle concept could result in major improvements in the over all nozzle performance characteristics.

REFERENCES

1. Luidens, R. W., Turney, G. E., and Allen, J., "Comparison of Two Parallel/Series Flow Turbofan Propulsion Concepts for Supersonic V/STOL," AIAA Paper 81-2637, Dec. 1981.

2. Boruff, W. R., and Roch, A. J., "Impact of Mission Requirements on V/STOL Propulsion Concepts Selection," Journal of Aircraft, Vol. 18, No. 1, Jan. 1981, pp. 43-50.

3. Burstadt, P. L., and Johns, A. L., "Experimental Results of a Deflected Thrust V/STOL Nozzle Research Program," AIAA Paper 83-0170, Jan. 1983.

Figure 1. - Reverse flow dual fan supersonic VSTOL aircraft configuration. Propulsion system shown in the vertical takeoff and landing mode.

+ FAN BLADES IN NORMAL PITCH
- FAN BLADES IN REVERSE PITCH

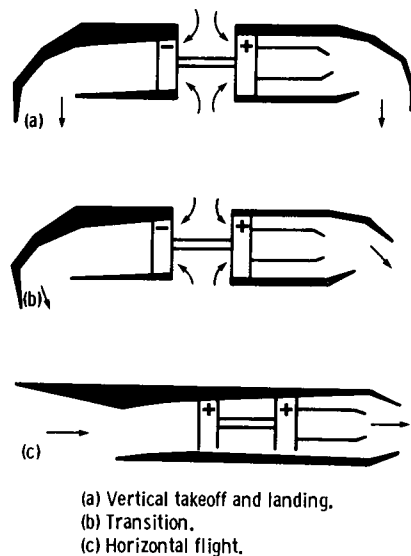(a) Vertical takeoff and landing.
(b) Transition.
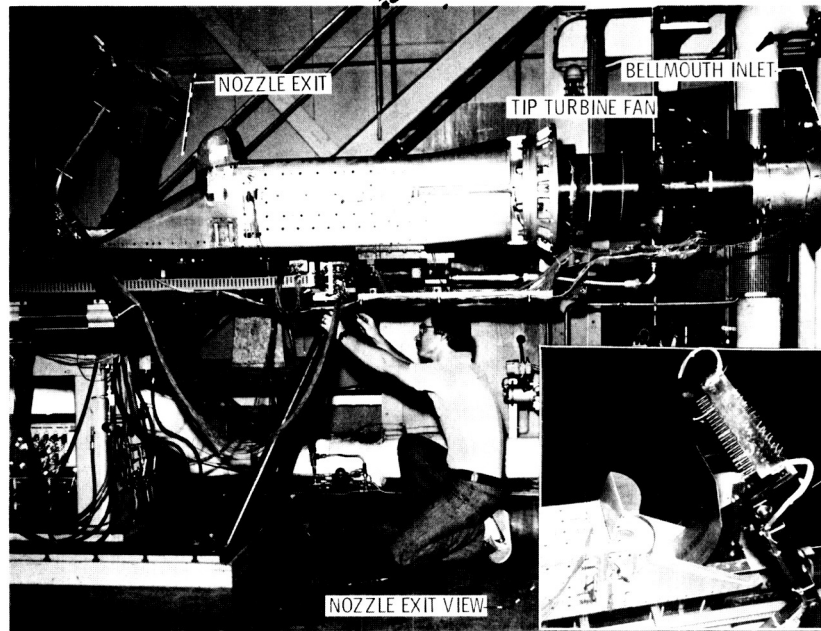(c) Horizontal flight.

Figure 2. - Propulsion system operation.

Figure 3. - 2-D inlet/nozzle installed in the vertical thrust stand.
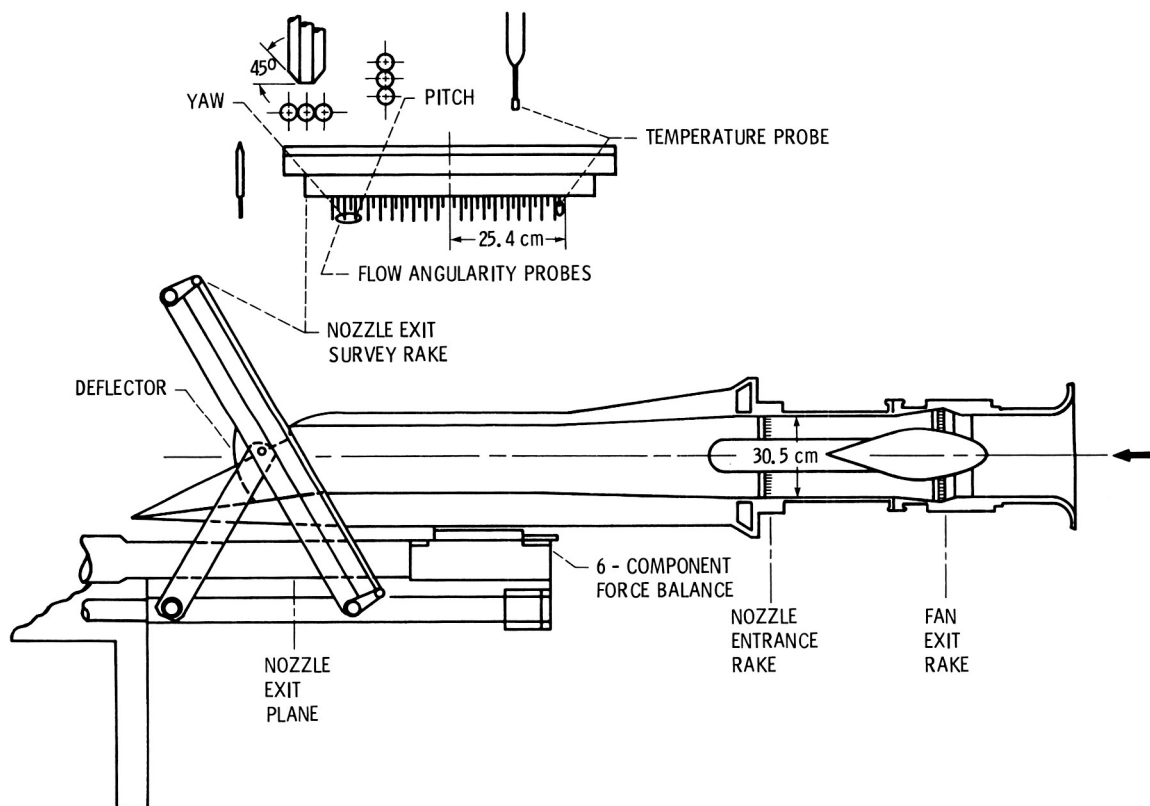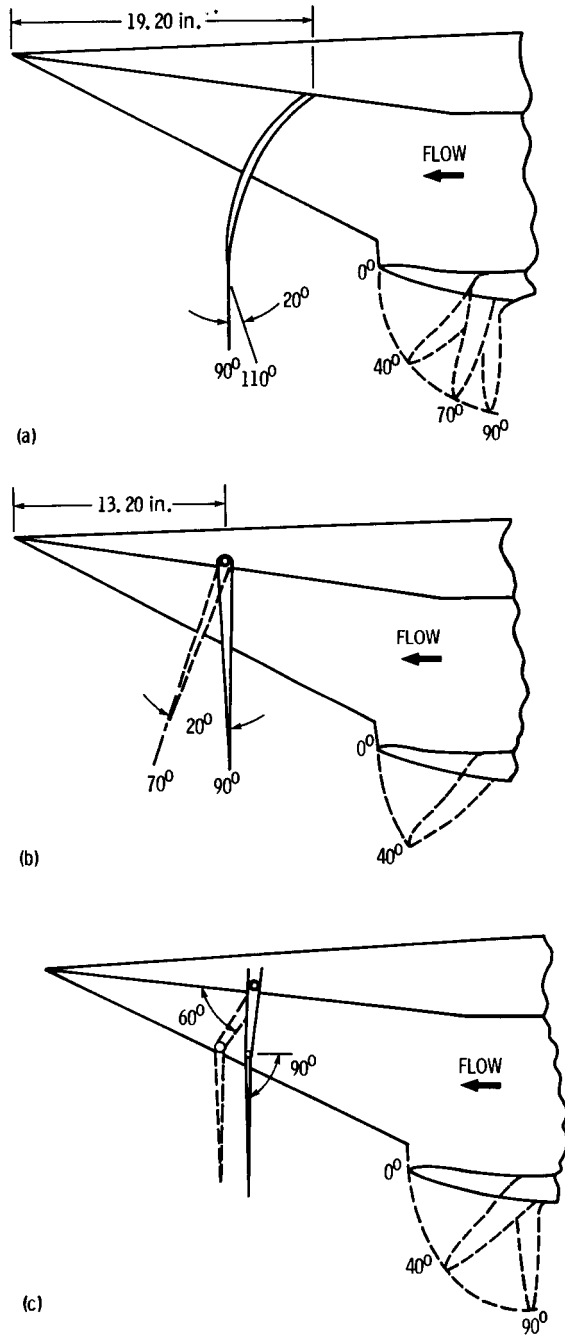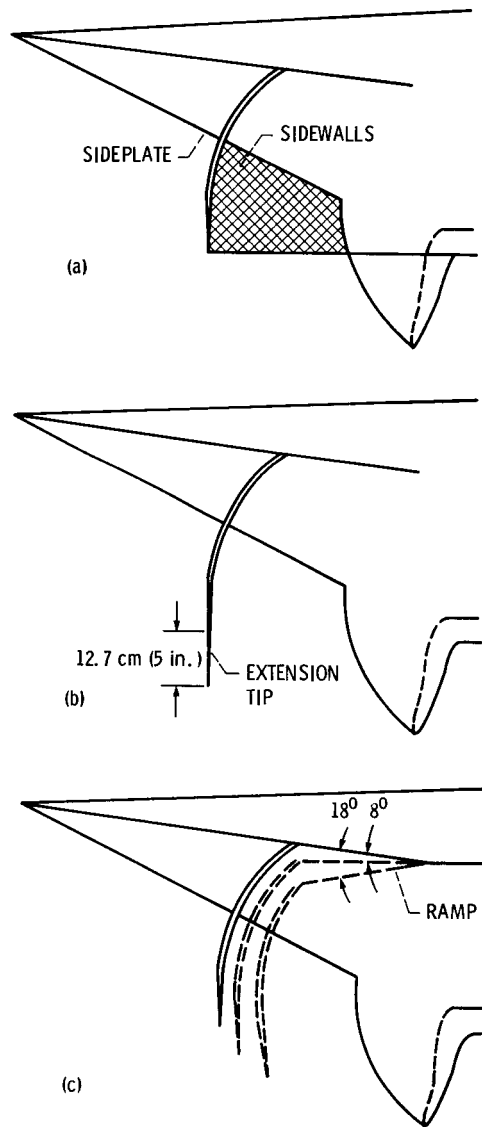

Figure 4. - Schematic of model installation and survey rake.

(a) Circular arc deflector.
(b) Single hinge deflector.
(c) Double hinge deflector.

Figure 5. - Model configurations.

(a) Sidewalls.
(b) Tip extension.
(c) Ramps.

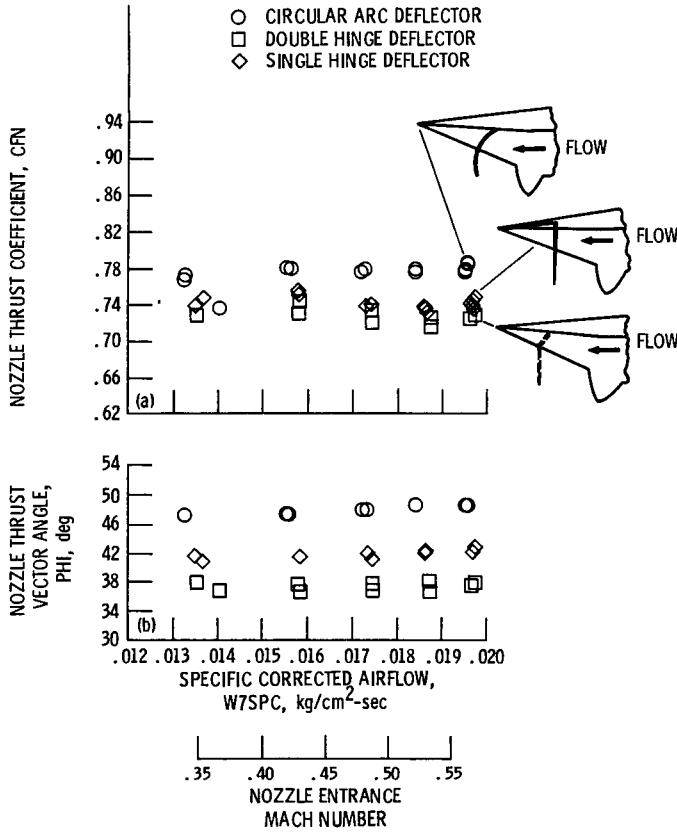Figure 6. - Configuration modifications. (Shown for circular arc deflector configuration.)

O CIRCULAR ARC DEFLECTOR
□ DOUBLE HINGE DEFLECTOR
◇ SINGLE HINGE DEFLECTOR

(a) Nozzle thrust coefficient.
(b) Nozzle thrust vector angle.

Figure 7. - Baseline performance with -8°
ramp, 40° droop lip, 90° flap angle.

DROOP
LIP
ANGLE

O 0°
□ 40°
◇ 70°

(a) Nozzle thrust coefficient.
(b) Nozzle thrust vector angle.
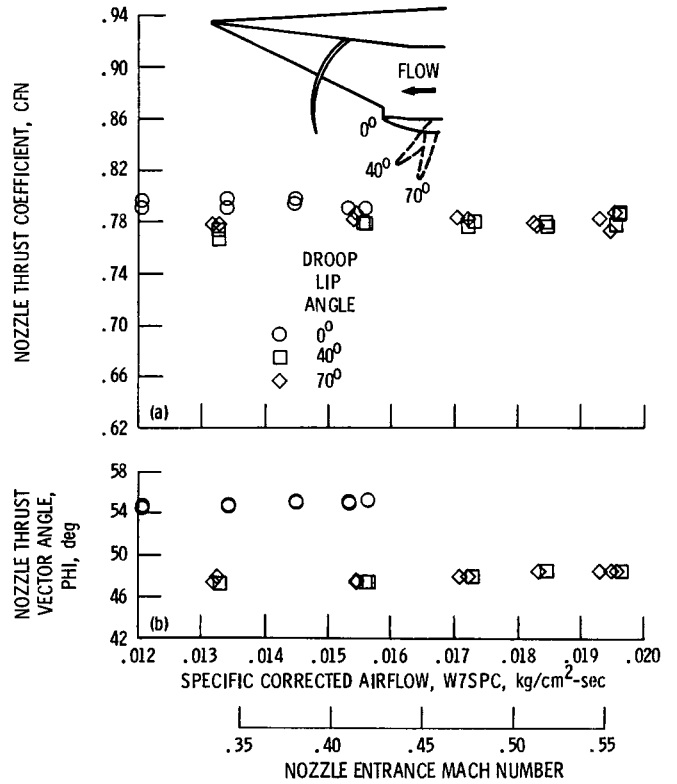
Figure 8. - The effect of droop lip. Circular arc deflector, -8°
ramp, 90° deflection.

SINGLE-HINGED DEFLECTOR

CIRCULAR ARC DEFLECTOR

DOUBLE-HINGED DEFLECTOR
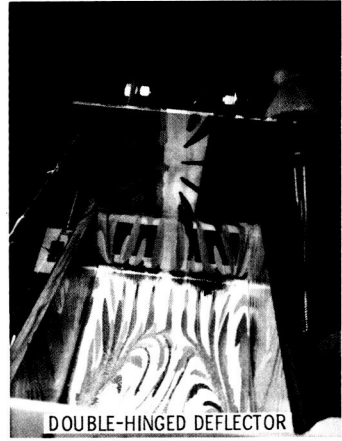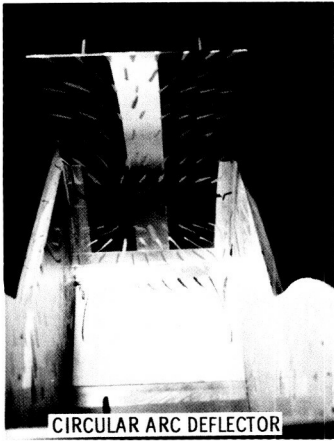
Figure 9. - Flow visualization for the baseline configuration showing side flow.

(a) Nozzle thrust coefficient.
(b) Nozzle thrust vector angle.
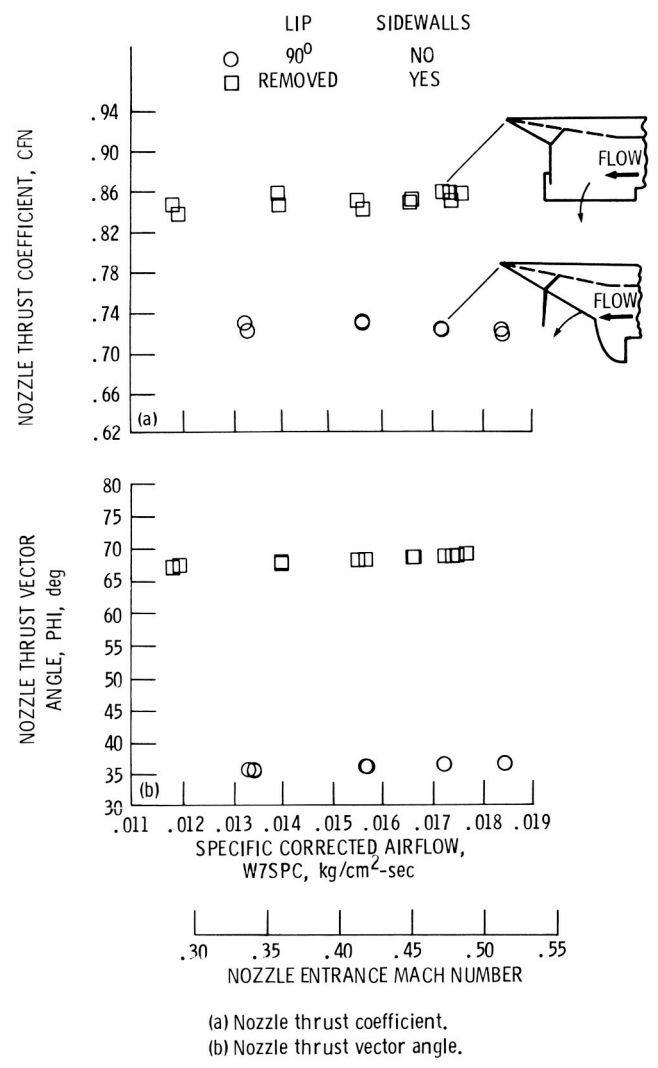
Figure 10. - The effect of sidewalls on nozzle performance. Double-hinged deflector, -8^0 ramp, 60^0 - 90^0 flap angle, nozzle exit area ratio, 1.76.
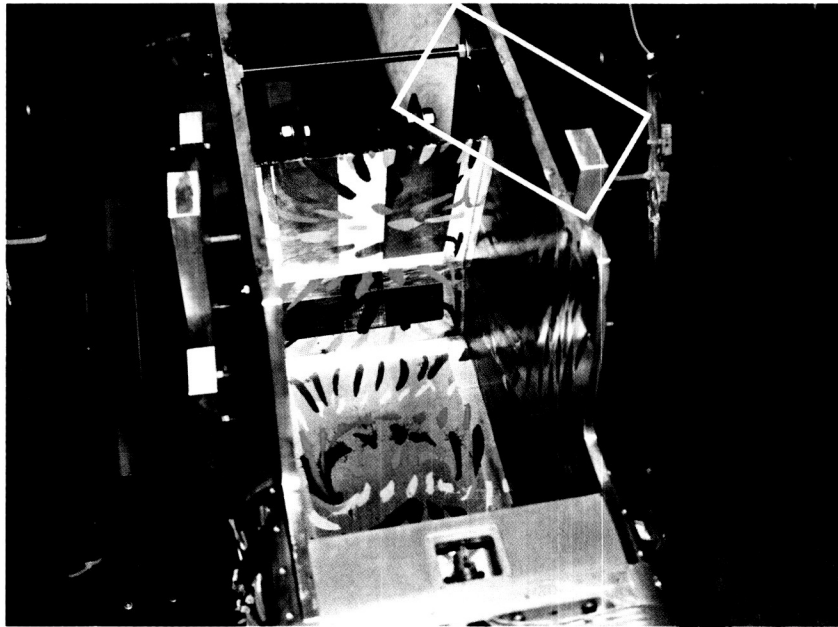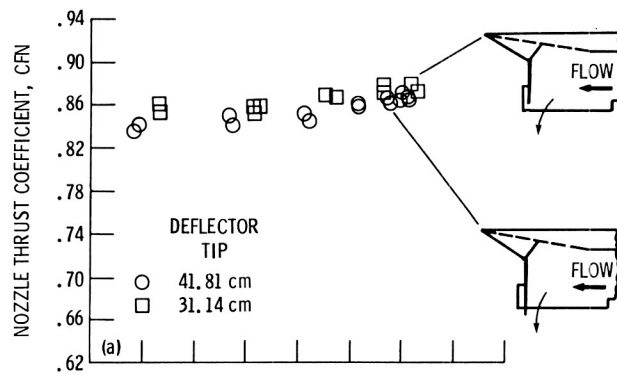
Figure 11. - Flow visualization with double-hinged deflector (60°-90°) showing aft flow on the sidewalls at the deflector tip.
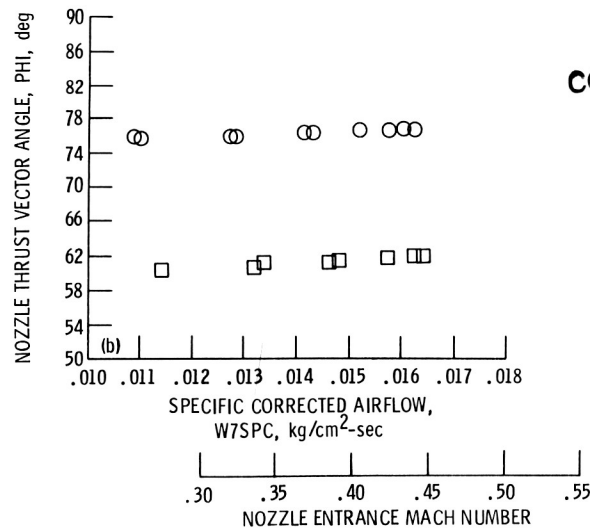
(a) Nozzle thrust coefficient.
(b) Nozzle thrust vector angle.

Figure 12. - The effect of deflector flap extension. Double-hinged deflector, -8° ramp, 60°-90° flap angles, lip removed.
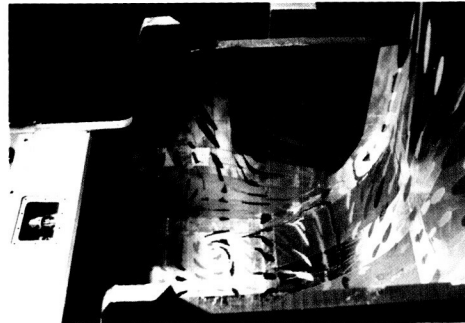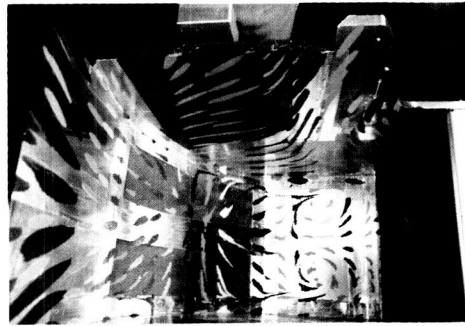
9

Figure 13. - Flow visualization results showing vortices on the -8⁰ ramp.

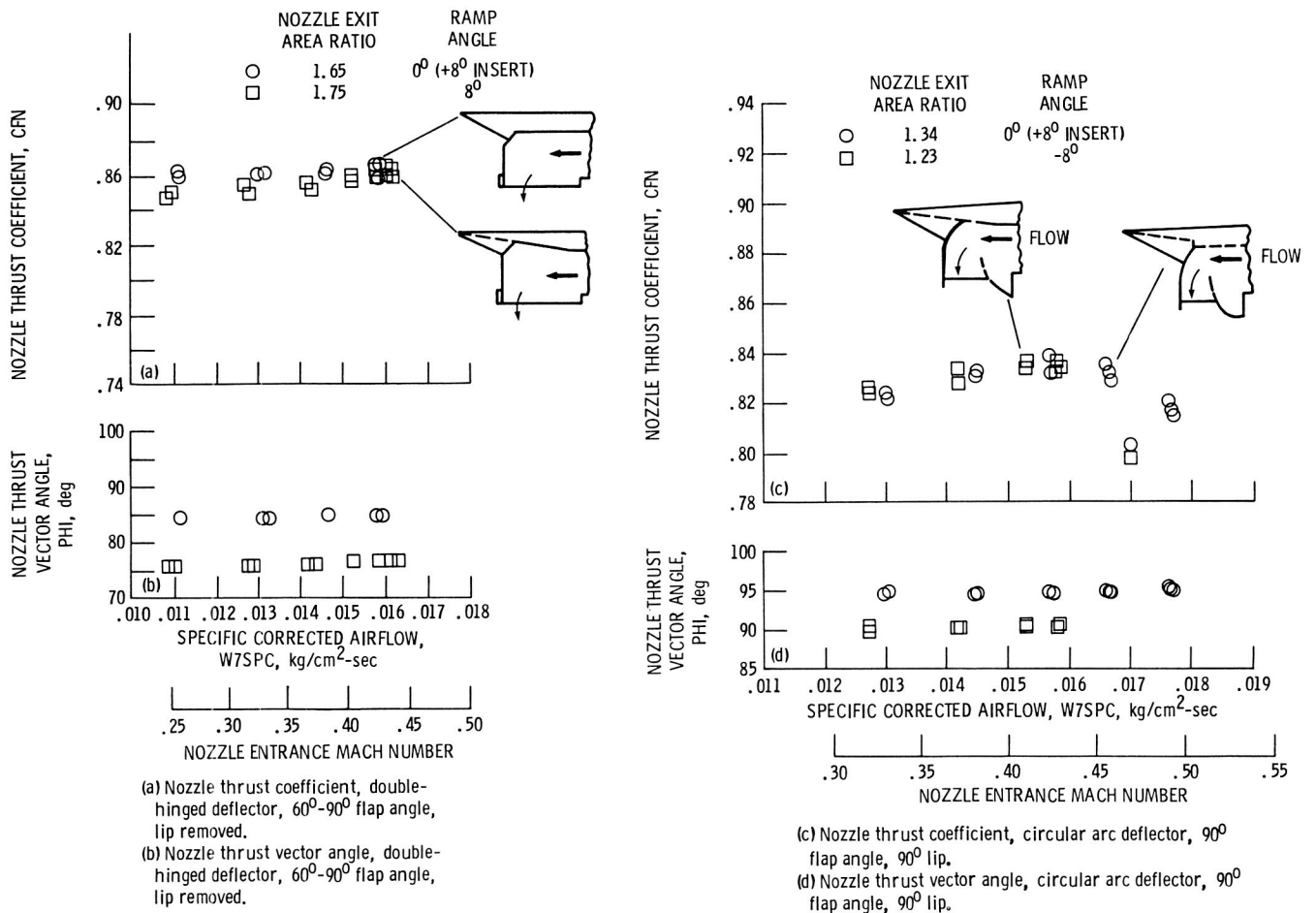(a) Nozzle thrust coefficient, double-hinged deflector, 60⁰-90⁰ flap angle, lip removed.
(b) Nozzle thrust vector angle, double-hinged deflector, 60⁰-90⁰ flap angle, lip removed.
(c) Nozzle thrust coefficient, circular arc deflector, 90⁰ flap angle, 90⁰ lip.
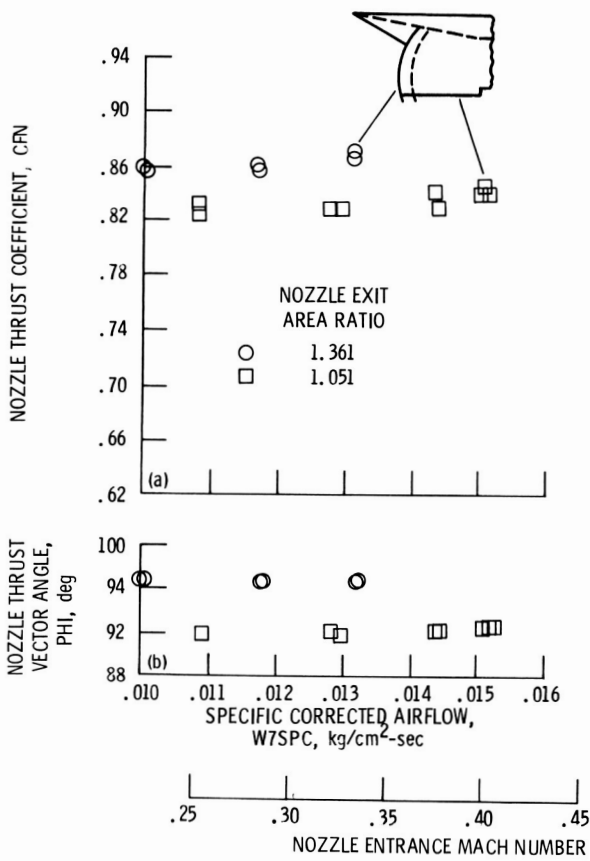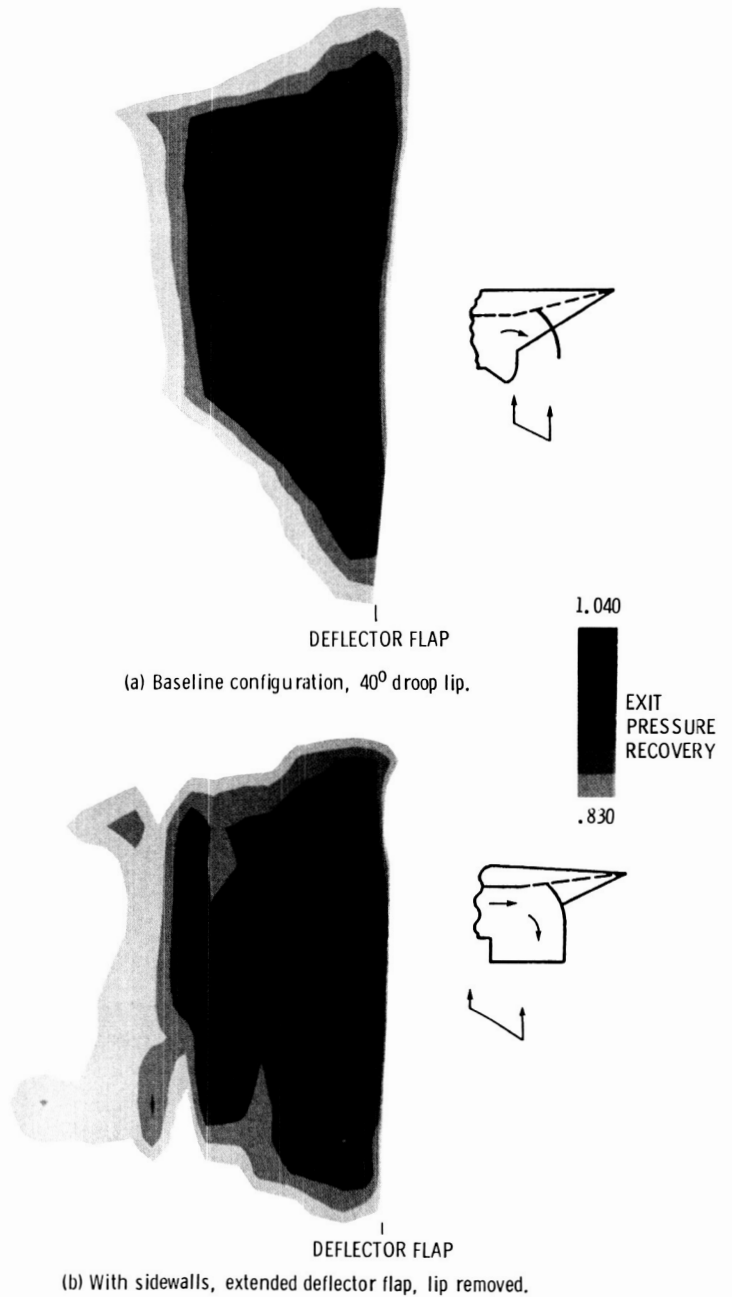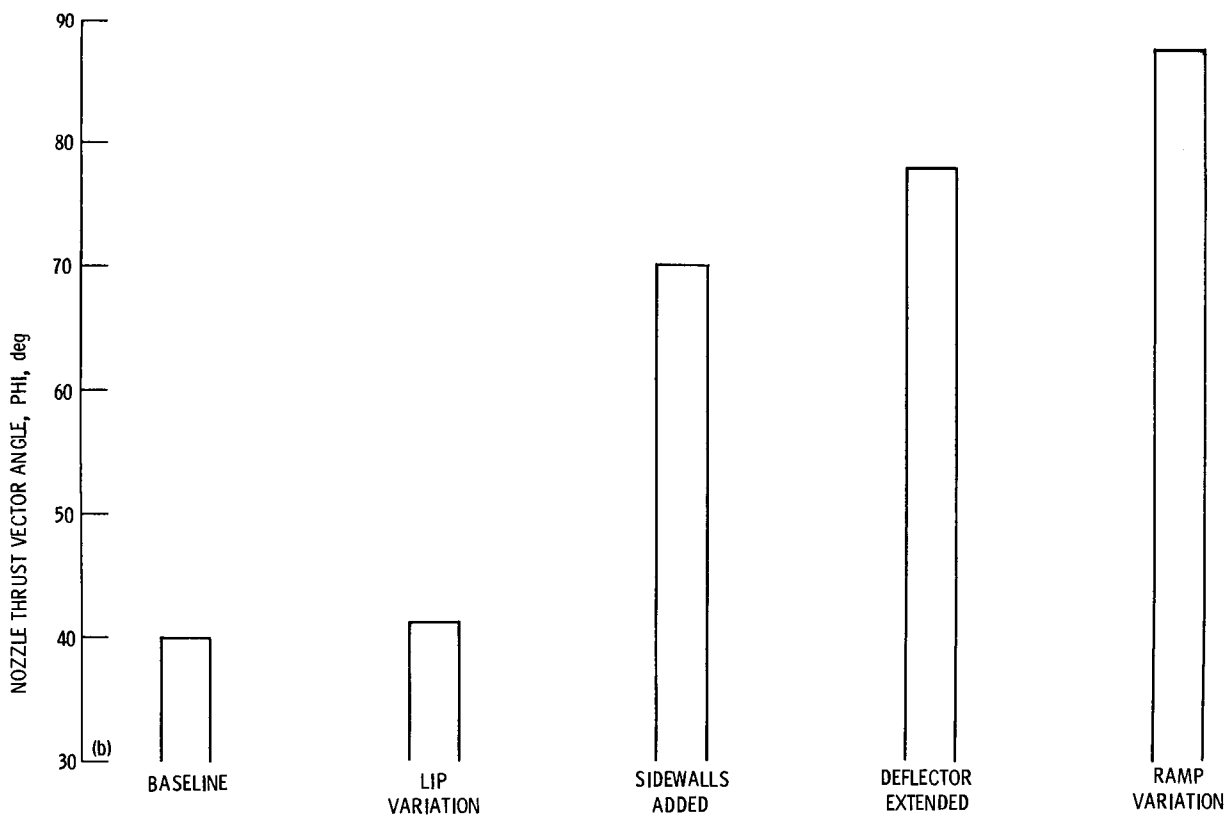(d) Nozzle thrust vector angle, circular arc deflector, 90⁰ flap angle, 90⁰ lip.

Figure 14. - The effect of ramp modification on nozzle performance characteristics.

10

(a) Baseline configuration, 40° droop lip.

EXIT
PRESSURE
RECOVERY

1.040

.830

(b) With sidewalls, extended deflector flap, lip removed.

DEFLECTOR FLAP

Figure 16. - Total pressure contour maps in nozzle exit flow. Circular arc deflector; specific corrected airflow, 0.014 kg/sec-ft², -8° ramp.

(a) Nozzle thrust vector angle, circular arc deflector.

(b) Nozzle thrust vector angle.

Figure 15. - The effect of nozzle exit area on nozzle performance characteristics. Circular arc deflector, -8° ramp, 100° flap angle.

11
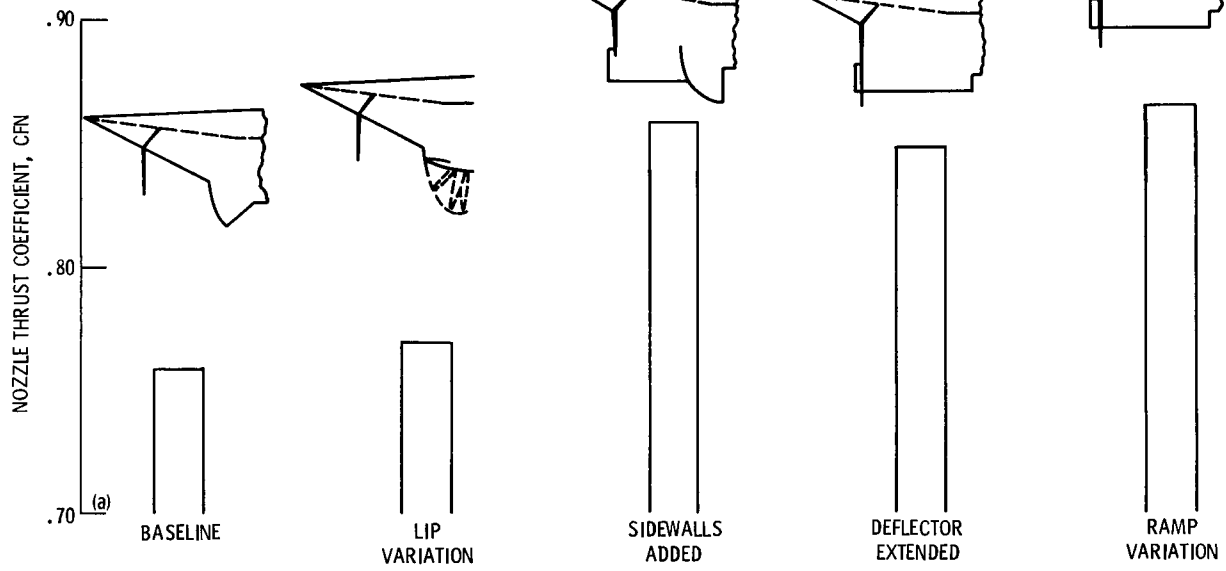
(a) Nozzle thrust coefficient.
(b) Nozzle thrust vector angle.

Figure 17. - Performance summary.

1. Report No. NASA TM-83439	2. Government Accession No.	3. Recipient's Catalog No.
4. Title and Subtitle Experimental Results for a Two-Dimensional Supersonic Inlet Used as a Thrust Deflecting Nozzle		5. Report Date
		6. Performing Organization Code 505-43-02
7. Author(s) Albert L. Johns and Paul L. Burstadt		8. Performing Organization Report No. E-1737
		10. Work Unit No.
9. Performing Organization Name and Address National Aeronautics and Space Administration Lewis Research Center Cleveland, Ohio 44135		11. Contract or Grant No.
		13. Type of Report and Period Covered Technical Memorandum
12. Sponsoring Agency Name and Address National Aeronautics and Space Administration Washington, D.C. 20546		14. Sponsoring Agency Code

15. Supplementary Notes

16. Abstract

Nearly all supersonic V/STOL aircraft concepts are dependent on the thrust deflecting capability of a nozzle. In one unique concept, referred to as the reverse flow dual fan, not only is there a thrust deflecting nozzle for the fan and core engine exit flow, but because of the way the propulsion system operates during vertical take-off and landing, the supersonic inlet is also used as a thrust deflecting nozzle. This paper presents results of an experimental study to evaluate the performance of a supersonic inlet used as a thrust deflecting nozzle for this reverse flow dual fan concept. Results are presented in terms of nozzle thrust coefficient and thrust vector angle for a number of inlet/nozzle configurations. Flow visualization and nozzle exit flow survey results are also shown.

17. Key Words (Suggested by Author(s)) Nozzle; Deflected thrust; V/STOL nozzles; Supersonic	18. Distribution Statement

19. Security Classif. (of this report) Unclassified	20. Security Classif. (of this page) Unclassified	21. No. of pages 13	22. Price* A02